International Scholarly Research Network
ISRN Civil Engineering
Volume 2012, Article ID 436327, 13 pages
doi:10.5402/2012/436327

Research Article

Some Studies on Prestressed Reinforced Granular Beds Overlying Weak Soil

J. Jayamohan and R. Shivashankar

Department of Civil Engineering, National Institute of Technology Karnataka, Mangalore 575025, India

Correspondence should be addressed to J. Jayamohan, jayamohan7@gmail.com

Received 25 July 2012; Accepted 12 September 2012

Academic Editors: G. C. Hart and I. Smith

This paper mainly investigates, from a series of laboratory scale bearing capacity tests carried out on a model square footing, the improvement in bearing capacity and reduction in settlement of a geonet reinforced granular bed (RGB) overlying weak soil due to prestressing the reinforcement. The parameters are the strength of the underlying weak soil, thickness of the granular bed, magnitude and direction of prestressing force. The settlements at the interface are also measured. The addition of prestress to geonet reinforcement results in significant improvement in the load carrying capacity and settlement response of the prestressed geonet RGB. Improvement in bearing capacity is found to be more with biaxial prestressing than with uniaxial prestressing. Experimental results are also used to validate a proposed numerical model. The BCR (bearing capacity ratio) values predicted from this model are found to be in good agreement with the experimentally obtained BCR values. Finite element analyses are also carried out using the programme PLAXIS, to study the effect of prestressing the reinforcement. Results obtained from finite element analyses are also found to be in good agreement with the experimental results.

1. Introduction

Soil reinforcing technique, using geosynthetics, has become a major ground improvement technique in geotechnical practice over the last three decades [1]. Its use is growing rapidly as worldwide development of infrastructure poses an increasing demand for land reclamation and utilization of soft foundation soils. Placing a granular bed over weak soil is the simplest technique of ground improvement that reduces settlements and increases bearing capacity of weak soil. The use of geosynthetic reinforced granular bed (RGB) over weak soil further reduces settlement and increases the bearing capacity of weak soil.

Many experimental and analytical studies have been performed to investigate the behaviour of reinforced granular beds for different soil types. Binquet and Lee [2] conducted tests on sand reinforced with metal strips. Shivashankar et al. [3] proposed that the improvement in bearing capacity of a reinforced granular bed is comprised of three components, namely, shear layer effect, confinement effect and surcharge effect. They proposed equations for computing the effect of each of these components. Kurian et al. [4] simulated reinforced soil systems with horizontal layers of reinforcement using a 3D nonlinear finite element programme. The results of numerical analysis were in good agreement with those obtained from model tests. Deb et al. [5, 6] presented a model for the analysis of granular foundation beds reinforced with several geosynthetic layers. The granular bed was modeled by Pasternak shear layer and geosynthetic reinforcement layers by stretched rough elastic membranes. The soft soil was represented by a series of nonlinear springs. An iterative finite difference scheme was applied for obtaining the solution and results were presented in nondimensional form.

Alamshahi and Hataf [7] studied the effect of providing grid anchors to geogrid in a reinforced sand slope. They conducted a series of laboratory model tests and finite element analysis of a strip footing resting on a reinforced sand slope. They found that the bearing capacity of rigid strip footings resting on reinforced slopes can be significantly increased by adding grid anchors to the reinforcement. Madhavilatha and Somwanshi [8, 9] conducted laboratory

model tests and numerical simulations on square footing resting on sand bed reinforced with different types of geosynthetics. The parameters studied were the type and tensile strength of reinforcement, depth of reinforced zone, spacing of geosynthetic layers, and the width of reinforcing layers. They found that, apart from the tensile strength of reinforcement, its layout and configuration play a vital role in improving the bearing capacity.

Sharma et al. [10] examined the existing analytical methods for the determination of bearing capacity of reinforced soil foundations. They conducted extensive laboratory and field tests on reinforced soil foundations resting over sandy and silty soils. They also conducted theoretical analysis and proposed the failure mechanism and equations for determination of bearing capacity considering also the tension developed in the reinforcement. Vinod et al. [11] conducted laboratory model tests to determine the improvement in bearing capacity and reduction in settlement of loose sand due to the addition of braided coir rope reinforcement. The results of their model tests indicated that bearing capacity can be increased by up to six times and settlement can be reduced by 90% by the introduction of coir rope reinforcement.

It is now well established that geosynthetics demonstrate their beneficial effects only after considerable settlements, since the strains occurring during initial settlements are insufficient to mobilize significant tensile load in the geosynthetic. This is not a desirable feature for foundations of certain structures, since their permissible values of settlement are small. Thus there is a need for a technique which will allow the geosynthetic to increase the load bearing capacity of soil without the occurrence of large settlements. The settlements of a reinforced granular bed can be considerably reduced by prestressing the geosynthetic reinforcement. Lovisa et al. [12] conducted laboratory model studies and finite element analysis on a circular footing resting on sand reinforced with geotextile. The improvement in bearing capacity due to prestressing the reinforcement was studied. It was found that the addition of prestress resulted in significant improvement in the load bearing capacity and reduction in settlement of foundation.

The purpose of this paper is to study experimentally the effects of prestressing the reinforcement in granular bed on the load-bearing capacity and settlement response of a reinforced granular bed overlying weak soil and to develop a numerical model to predict the extent of improvement. The study involved laboratory scale model tests on a square footing of size 100 × 100 × 20 mm thick. The parameters studied are the effects of the strength of the underlying weak soil, thickness of granular bed, magnitude of prestress, direction of prestress, and submergence of weak soil. The settlement at the interface between weak soil and GB is also measured. A nonlinear finite element analysis is conducted using the FE programme PLAXIS version 8 and the results are compared with those obtained from the model tests.

2. Experimental Programme

The experimental programme mainly involved a series of laboratory scale bearing capacity tests conducted on a model footing resting on a prestressed reinforced granular bed overlying weak soil. Details of the experimental programme, test procedures, and analyses of test results are presented in the following sections.

Table 1: Properties of sand used in the model tests.

Property	Value
Specific gravity	2.61
Average dry unit weight during model test (KN/m^3)	16.60
Void ratio during model test	0.54
Effective grain size D_{10} (mm)	0.50
D_{60} (mm)	1.30
D_{30} (mm)	0.80
Coefficient of uniformity C_u	2.60
Coefficient of curvature C_c	1.00
Friction angle Φ°	31.0
Cohesion (kPa)	0
Relative density	0.86

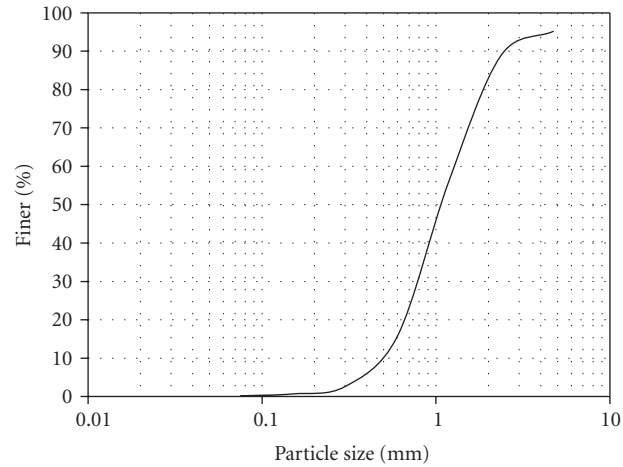

Figure 1: Particle size distribution of sand used in model test.

2.1. Materials. The material used for granular bed is sand and its properties are given in Table 1 and particle size distribution is shown in Figure 1. Locally available silty soil termed as "Shedi soil" is used as weak soil and its properties are given in Table 2 and particle size distribution is shown in Figure 2. The shedi soil is used in two conditions, namely, moist condition (termed as moist soil or weak soil 1) and in submerged condition (termed as submerged soil or weak soil 2). The reinforcement used is geonet and its properties are given in Table 3.

Shedi soils are predominantly found in the west coast (Konkan coast) of southern peninsular India and most of the foundations are placed on this soil layer. These soils are problematic in the sense that their strength reduces drastically under saturation condition, which is the typical behaviour of dispersive type of soils. It has resulted in many foundation problems wherever it is met with.

Table 2: Properties of weak soil used in model tests.

Property	Value
Specific Gravity	2.32
Average dry unit weight during model test (KN/m^3)	16.00
Void ratio during model test	0.42
Effective grain size D_{10} (mm)	0.11
Shear parameters of (moist) weak soil 1 (water content = 10%)	
Friction angle Φ°	12
Cohesion (kPa)	10
Shear parameters of (submerged) weak soil 2 (water content = 31.5%)	
Friction angle Φ°	6
Cohesion (kPa)	5.5
Liquid limit (%)	37.4
Plastic limit (%)	32.9
Shrinkage limit (%)	25.7

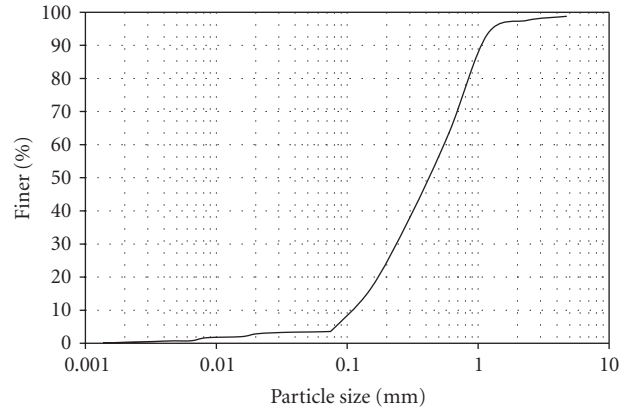

Figure 2: Particle size distribution of weak soil used in model test.

2.2. Test Setup. Laboratory scale bearing capacity tests are carried out on a square rigid footing made of mild steel. The dimensions of the model footing are 100 mm × 100 mm × 20 mm thick. The model footing is kept on the surface of soil during all the tests.

The test tank is made of ferrocement having internal dimensions 0.75 m × 0.75 m in plan and 0.75 m high. A single layer of reinforcement is used. The prestress applied is equal to 1%, 2%, and 3% of the tensile strength of the geonet and is distributed over three pulleys. In uniaxial prestressing, the prestress is applied only in the X-direction, whereas in biaxial prestressing it is applied in both X and Y directions as shown in Figures 3 and 4, respectively. The test setup is shown in Figure 5 and photograph of it is shown in Figure 6.

The load is applied using a hydraulic jack of 10 KN capacity. The load is measured using a proving ring and deformation using two dial gauges placed diametrically opposite to each other. Preparation of underlying soil in all the tests involved compaction of soil using a rammer. In the preparation of foundation (granular) bed, the sand is compacted using a small plate vibrator. The densities to which the soils were compacted are indicated in Tables 1 and 2.

Table 3: Properties of geonet used in model tests.

Property	Value
Mass per unit area (gm/m^2)	730.00
Aperture size (mm)	8 × 6
Thickness (mm)	3.30
Tensile strength (KN/m)	7.68
Extension at maximum load (%)	20.20
Colour	Black
Polymer	HD-polyethylene

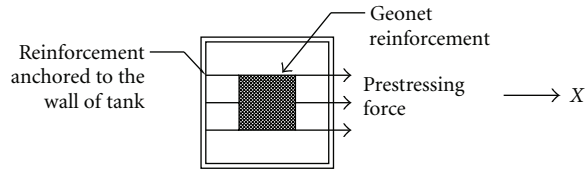

Figure 3: Uniaxial prestressing.

In the literature it is reported that optimum depth of placement of the first layer of reinforcement is 0.2 B to 0.5 B (B is the width of footing) [10]. The depth of reinforcement from the base of footing was adopted as 0.5 B for all the tests. Same procedure and same compactive effort are used in all the tests to maintain consistency and for sake of comparison.

2.3. Test Details. At first, the weak silty soil is filled in the ferrocement tank to the required level with compaction made in layers, to achieve the predetermined density. Then sand is filled up to the bottom level of reinforcement and compacted. The reinforcement is then placed with its centre exactly beneath the jack and prestress is applied. Then sand above the reinforcement is placed and compacted to the predetermined density.

The compactive effort required to achieve the required density of both soils is determined by trial and error. The settlement is measured using two dial gauges and their average value is adopted. The settlement at the interface between two soils is determined by measuring the levels at specified points at regular intervals on the surface of weak soil before and after each test. The test tank is emptied and refilled for each test to ensure that controlled conditions are maintained throughout the investigation. A total of 34 tests are conducted. The details of testing programme are shown in Table 4.

Under series A, tests were conducted on weak soil 1 (moist soil) and on weak soil 1 overlain with unreinforced granular bed of thickness B or $2B$. Under series B, tests were conducted on weak soil 1 overlain with reinforced granular bed of thickness B or $2B$. Under series C, tests were conducted on weak soil 1 overlain with prestressed reinforced granular bed. The prestress applied was uniaxial. The parameters varied were magnitude of prestress and thickness of granular bed. Series D was similar to series C

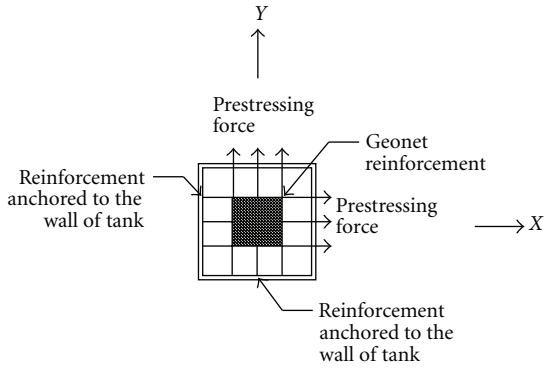

Figure 4: Biaxial prestressing.

except that prestress applied was biaxial. Series E, F, G, and H are similar to series A, B, C, and D, respectively, except that the underlying soft soil was kept submerged (termed as weak soil 2). The level of water table was monitored by installing four piezometers.

3. Numerical Analysis

3.1. Punching Shear Model of Strip Footing [3]. Shivashankar et al. [3] developed a punching shear model for a strip footing on unreinforced or reinforced granular bed overlying weak soil. They proposed a punching shear failure mechanism in which both the footing and the portion of the reinforced granular bed directly beneath the footing are envisaged to act in unison to punch through the soft soil underneath.

The improvement in bearing capacity of a reinforced granular bed was considered to comprise of three components, namely, shear layer effect, confinement effect, and surcharge effect. These effects are represented in Figures 7, 8, and 9, respectively. They proposed the following equations for computing bearing capacity ratio (BCR):

$$\mathrm{BCR} = 1 + \Delta\mathrm{BCR}_{\mathrm{SL}} + \Delta\mathrm{BCR}_{\mathrm{CE}} + \Delta\mathrm{BCR}_{\mathrm{SE}}, \tag{1}$$

where bearing capacity ratio (BCR) is defined as ratio of bearing capacity of footing on improved ground to bearing capacity of footing on unimproved ground. $\Delta\mathrm{BCR}_{\mathrm{SL}}$, $\Delta\mathrm{BCR}_{\mathrm{CE}}$, and $\Delta\mathrm{BCR}_{\mathrm{SE}}$ are improvements in bearing capacity ratio due to shear layer effect, confinement effect, and additional surcharge effect, respectively.

3.1.1. Shear Layer Effect. In shear layer effect, the shear stress mobilized along the failure surfaces (vertical planes at the edge of the footing) due to the passive pressure developed in granular soil is considered (Figure 7). The equation proposed for strip footings is

$$\begin{aligned} \Delta\mathrm{BCR}_{\mathrm{SL}} &= 2\tau_1/Q, \\ \tau_1 &= P_p \tan\phi_s, \\ \Delta q_{\mathrm{SL}} &= 2\tau_1/B, \end{aligned} \tag{2}$$

where Q = bearing capacity of underlying weak soil, τ_1 = total vertical force in the punching shear failure (vertical) plane due to shear layer effect, P_p = passive force developed on the sides of failure surface per unit length, and ϕ_s = angle of shearing resistance.

3.1.2. Confinement Effect. The tensile stress mobilized in the reinforcement (placed in the granular soil) will provide a confinement effect to the granular soil beneath the footing. The shear stress developed along the failure surfaces (vertical planes at the edge of the footing) due to this confining stress is considered here (Figure 8). The equation proposed for strip footing was

$$\Delta\mathrm{BCR}_{\mathrm{CE}} = 2\tau_2/Q, \tag{3}$$

$$\tau_2 = T_R \tan\phi_s, \tag{4}$$

$$\Delta q_{\mathrm{CE}} = 2\tau_2/B, \tag{5}$$

where τ_2 = total vertical force in the punching shear failure plane (vertical) due to confinement effect of reinforcement, T_R = tensile stress mobilized in the reinforcement = $2L\sigma_v \tan\delta$, L = length of reinforcement beyond the failure surface, σ_v = vertical stress at the level of reinforcement, and δ = angle of friction between reinforcement and soil, taken as equal to ϕ_s for geonet.

3.1.3. Additional Surcharge Effect. The vertical stresses along the punching shear failure surfaces due to shear layer effect and confinement effect are considered to act as additional surcharge stress on the underlying soft soil. There will be an improvement in bearing capacity due to this additional surcharge stress. The distribution of this surcharge stress is envisaged to be exponential on either side from the edge of the footing as shown in Figure 9 for a strip footing. The improvement in bearing capacity due to this surcharge stress is given by:

$$q_o = 0.84\left(\Delta q_{\mathrm{SL}} + \Delta q_{\mathrm{CE}}\right), \tag{6}$$

where q_o = intensity of surcharge stress at the edge of the vertical failure plane (on weak soil), due to shear layer and confinement effects.

The effect of this additional surcharge, exponentially decreasing from q_o at the edge of the footing to $0.01q_o$, is used in analysis of improvement of bearing capacity, that is, in estimation of $\Delta\mathrm{BCR}_{\mathrm{SE}}$.

3.2. Modeling of Square Footing on Unreinforced or Reinforced Granular Beds (RGB) in the Present Study. In the present study, the model suggested by Shivashankar et al. [3] for strip footing has been modified and used for validating the results of a square footing on unreinforced or reinforced (without prestressing) granular beds, overlying weak soils. Equation (7) are adopted for shear layer effect. Equations (8) and (9) are adopted for confinement effect, in case of RGB. An exponentially decreasing surcharge as before is envisaged on all four sides, and the effect of this additional surcharge is

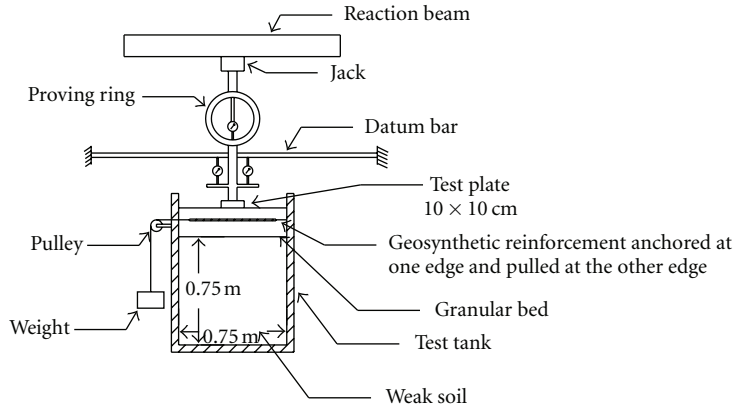

Figure 5: Test setup.

Table 4: Testing programme.

Series	Type	Thickness	Prestress	
			Direction	Magnitude
A	Weak soil 1 (moist soil)		—	—
	(Unreinforced) granular bed on weak soil 1	B & 2B	—	—
B	Reinforced granular bed on weak soil 1	B & 2B	—	—
C	Prestressed reinforced granular bed on weak soil 1	B & 2B	Uniaxial	1%, 2%, and 3%
D	Prestressed reinforced granular bed on weak soil 1	B & 2B	Biaxial	1%, 2%, and 3%
E	Unreinforced weak soil 2 (submerged soil)		—	—
	(Unreinforced) granular bed on weak soil 2	B & 2B	—	—
F	Reinforced granular bed on weak soil 2	B & 2B	—	—
G	Prestressed reinforced granular bed on weak soil 2	B & 2B	Uniaxial	1%, 2%, and 3%
H	Prestressed reinforced granular bed on weak soil 2	B & 2B	Biaxial	1%, 2%, and 3%

Figure 6: A view of the test setup.

used in analysis of improvement of bearing capacity, that is, estimation of ΔBCR_{SE}.

3.3. Modeling of Square Footing on Prestressed Reinforced Granular Beds in the Present Study. The model proposed by Shivashankar et al. [3] has been modified and improved for the case of square footings on prestressed reinforced granular beds overlying weak soils.

3.3.1. Shear Layer Effect. The following equations are used for a square footing of width "B":

$$\Delta BCR_{SL} = 4\tau_1/Q,$$
$$\tau_1 = P'_p \tan\phi_s, \tag{7}$$

where P'_p is the passive force developed on each of four sides of the square column of granular soil beneath the square footing.

3.3.2. Confinement Effect. Equations (3) and (4) for strip footing are modified for square footing as

$$\Delta BCR_{CE} = 4\tau_2/Q, \tag{8}$$

$$\tau_2 = T'_R \tan\phi_s, \tag{9}$$

where T'_R = tensile stress mobilized in reinforcement beyond each of the four sides of square column of granular soil beneath the square footing, and B = width of the square footing.

If the friction in reinforcement (on each side of the square prism) is less than the applied prestress, value of T'_R is taken as equal to the value of applied prestress. If the friction in reinforcement is more than applied prestress, the value of T'_R is taken as equal to value of frictional resistance over the reinforcement.

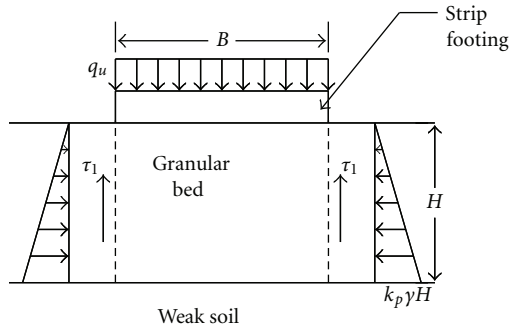

Figure 7: Shear layer effect [3].

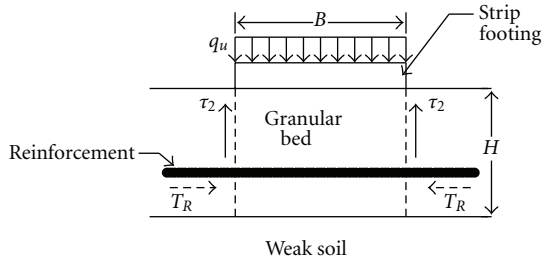

Figure 8: Confinement effect [3].

3.3.3. Additional Surcharge Effect. As explained in Sections 3.1.3 and 3.2, the vertical stresses along the punching shear (vertical) failure surface due to shear layer effect and confinement effect are considered to act as additional surcharge stress on the underlying weak soil. This effect will cause a further improvement in bearing capacity (ΔBCR_{SE}). Due to uniform tension in reinforcement due to prestressing, this additional surcharge stress is envisaged to be uniform over the area of reinforcement in the direction of prestressing (Figure 10). In uniaxial prestressing, the surcharge is considered to be uniform (q_s) over the area of reinforcement, in the direction of prestress. In the other perpendicular direction, it is considered to decrease exponentially from (q_o) at edge of footing and 0.01 (q_o) at the end of the reinforcement. Overall, an average surcharge (average of uniform surcharge in one direction and exponential decrease on the other side) is considered in perpendicular direction for estimation of ΔBCR_{SE}. In case of biaxial prestressing, the surcharge is considered to be uniform (q_s) over the area of reinforcement, in both X and Y directions. The following equations are used for biaxial case:

$$\Delta q_{SE} = q_s N_q, \tag{10}$$

where N_q is the bearing capacity factor and

$$\Delta BCR_{SE} = \Delta q_{SE}/Q,$$
$$q_s = [(\tau_1 + \tau_2) \cdot 2H]/(L - B). \tag{11}$$

4. Finite Element Analysis

In the present study, loading tests on reinforced granular beds are also simulated numerically using the programme

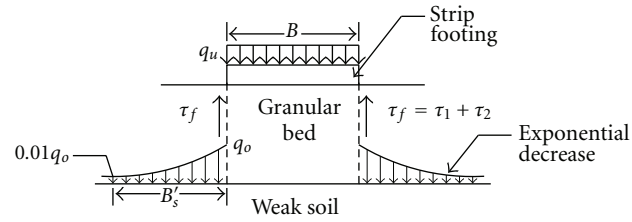

Figure 9: Additional surcharge effect [3].

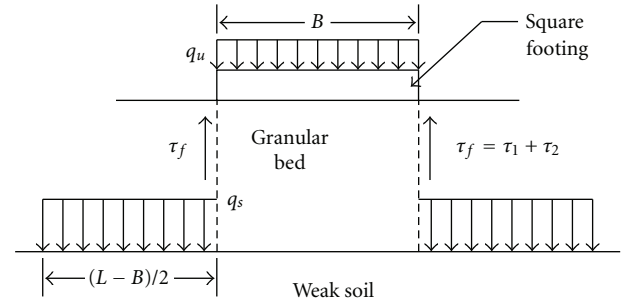

Figure 10: Proposed additional surcharge effect for prestressed RGB (square footing).

PLAXIS (version 8) which is a finite element software package. For simulating the behaviour of soil, different constitutive models are available. In the present study, Mohr-Coulomb model is used to simulate soil behaviour. This non linear model is based on the basic soil parameters that can be obtained from direct shear tests, internal friction angle, and cohesion intercept.

Due to symmetry of the soil-footing-reinforcement system, an axisymmetric model is used to carry out the finite element analysis. The settlement of the rigid footing is simulated using nonzero prescribed displacements. The outer boundaries of the mesh are of the same dimensions as the tank used for model tests. The displacement of the bottom boundary is restricted in all directions, while at the vertical sides, displacement is restricted only in the horizontal direction. The initial geostatic stress states for the analyses are set according to the unit weight of the test soil.

The soil is modeled using 15-nodded triangular elements. The modulus of elasticity E is different for each simulation due to the increase in strength of soil induced by reinforcement and prestress. The modulus of subgrade reaction is found out for each trial from the experimental data and then the modulus of elasticity is computed using the following relationship [13]:

$$E = k_s \cdot H(1 + \nu)(1 - 2\nu), \tag{12}$$

where E is the modulus of elasticity (kPa), k_s is modulus of subgrade reaction for soil (KN/m^3), H is thickness (m), and ν is Poisson's ratio. The value of H is determined by conducting a number of simulations and comparing the results with the experimental values. It is found out that a reasonably accurate value of E could be obtained when the values of H are between 2.5 and 3 times the width of footing. The value of Poisson's ratio is assumed to be 0.25 for all cases.

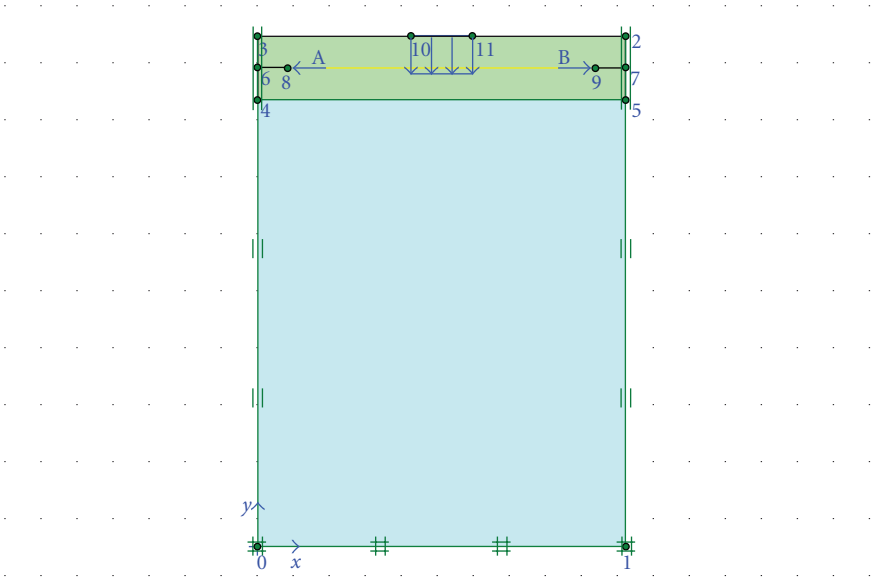

(a)

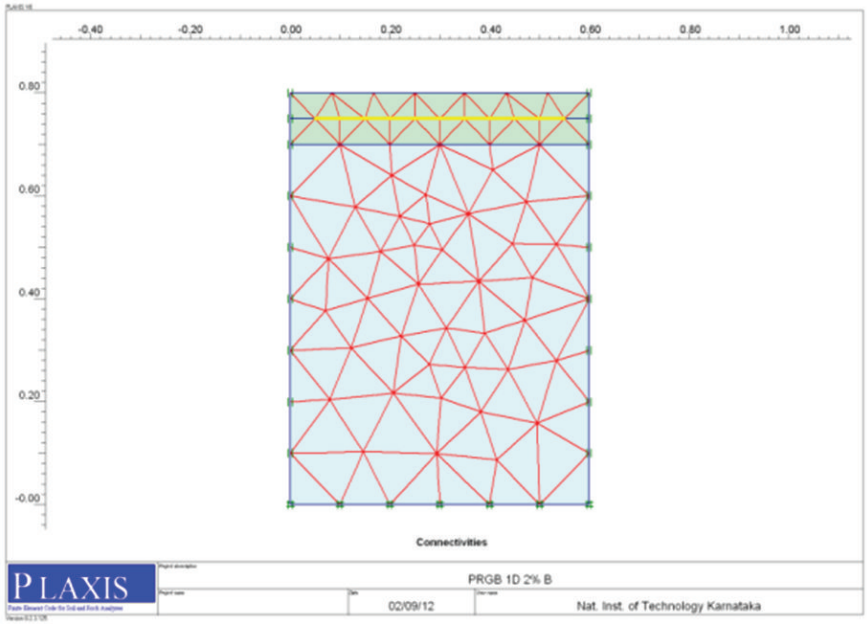

(b)

Figure 11: Geometric model and discretized model.

The reinforcement is modeled using the 5-nodded geogrid element. The material property required for reinforcement is elastic axial stiffness EA. To simulate the interaction between the reinforcement and surrounding soil, an interface element is provided on both upper and lower surface of reinforcement. The interaction between soil and reinforcement is simulated by choosing an appropriate value for strength reduction factor R_{inter} at the interface. The aperture size of geonet is sufficiently large enough to allow soil-to-soil contact through the apertures and hence the angle of friction between reinforcement and soil is taken equal to the angle of internal friction of sand Φ. Hence the value of R_{inter} is taken as one. The prestress is applied as a horizontal tensile load to the reinforcement (Figure 11).

Mesh generation can be done automatically. Medium mesh size is adopted in all the simulations. The discretized model is also shown in Figure 11. To simulate exactly the testing procedure in the laboratory, staged construction procedure is adopted in the calculation phase. In the first stage, weak soil up to its top level is simulated. In the second stage, sand up to the bottom level of reinforcement is simulated. In the third stage the reinforcement with prestress is simulated, and in the fourth stage sand above the reinforcement is simulated. In the final stage the footing with

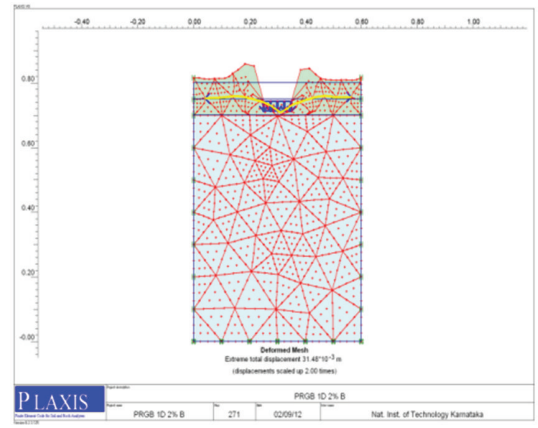

(a)

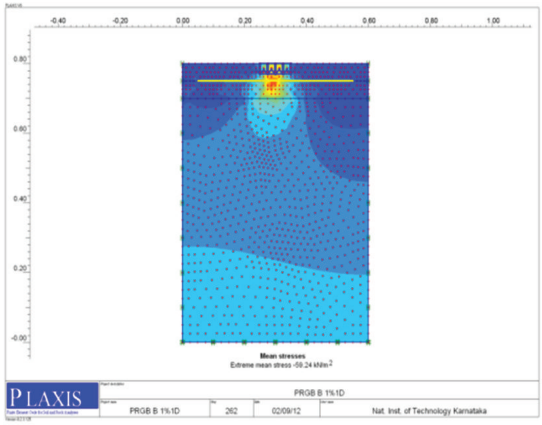

(b)

Figure 12: Deformed shape and stress distribution after loading.

prescribed displacement is simulated. Such a staged construction procedure is necessary because the reinforcement should be prestressed before filling soil above it, otherwise the friction between soil and reinforcement will prevent the elongation of reinforcement due to prestressing. The deformed shape and stress distribution in soil are shown in Figure 12.

5. Results and Discussions

5.1. Improvement in Bearing Capacity. Vertical stress (load per unit area) versus normalized settlement curves are shown in Figures 13 to 26. The footing settlement S is expressed in non dimensional form as S/B (%). It is clearly observed that the addition of prestress significantly improved the settlement behaviour of soil. The load carrying capacity of footing is also significantly improved. Load-settlement analysis from finite element analysis is also shown in these figures.

5.1.1. Effect of Magnitude of Prestress

Granular Beds Overlying (Moist) Weak Soil 1. From Figure 13 which represents the variation of bearing pressure with

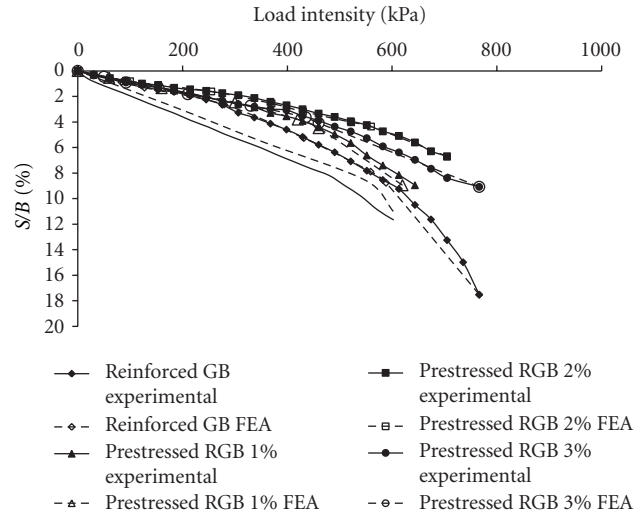

Figure 13: Load intensity versus normalized settlement curves for granular bed of thickness B with uniaxial prestressing overlying (moist) weak soil 1.

footing settlement of uniaxially prestressed granular bed of thickness B overlying (moist) weak soil 1, it can be seen that maximum improvement is observed when the magnitude of prestress was equal to 2% of the tensile strength of reinforcement. Further addition of prestress is not beneficial. However, for a granular bed of thickness B with biaxial prestressing overlying (moist) weak soil 1, it was observed that the maximum improvement in settlement behaviour occurred when the magnitude of prestress was equal to 1% of the tensile strength of reinforcement. Further increase in prestress is not beneficial (Figure 14).

The results obtained from a granular bed of thickness $2B$ with uniaxial prestressing overlying (moist) weak soil 1 is shown in Figure 15. It is observed that the maximum improvement is when the magnitude of prestress is equal to 3% of the tensile strength of reinforcement. The results obtained from a granular bed of thickness $2B$ with biaxial prestressing overlying (moist) weak soil 1 indicates that maximum improvement is obtained also when the magnitude of prestress is equal to 3% of the tensile strength of reinforcement (Figure 16).

Granular Beds Overlying (Submerged) Weak Soil 2. Figure 17 presents the variation of bearing pressure with footing settlement of uniaxially prestressed granular bed of thickness B overlying (submerged) weak soil 2. It can be seen that maximum improvement is observed when the magnitude of prestress is equal to 2% of the tensile strength of reinforcement. Further addition of prestress is found to be not beneficial. This is the same as in the case of weak soil 1.

In case of granular bed of thickness B with biaxial prestressing overlying submerged weak soil, from Figure 18, it is observed that the maximum improvement in settlement behaviour occurs when the magnitude of prestress is equal to 2% of the tensile strength of reinforcement. This is unlike the case of weak soil 1, which peaked at 1%, itself.

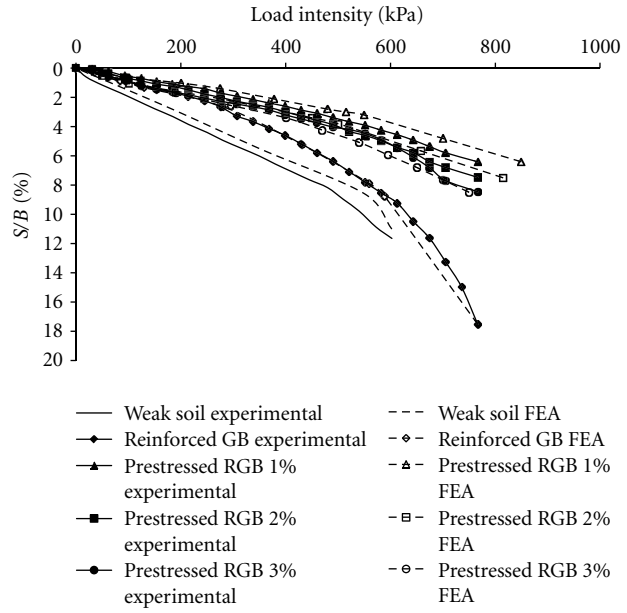

Figure 14: Load intensity versus normalized settlement curves for granular bed of thickness B with biaxial prestressing overlying (moist) weak soil 1.

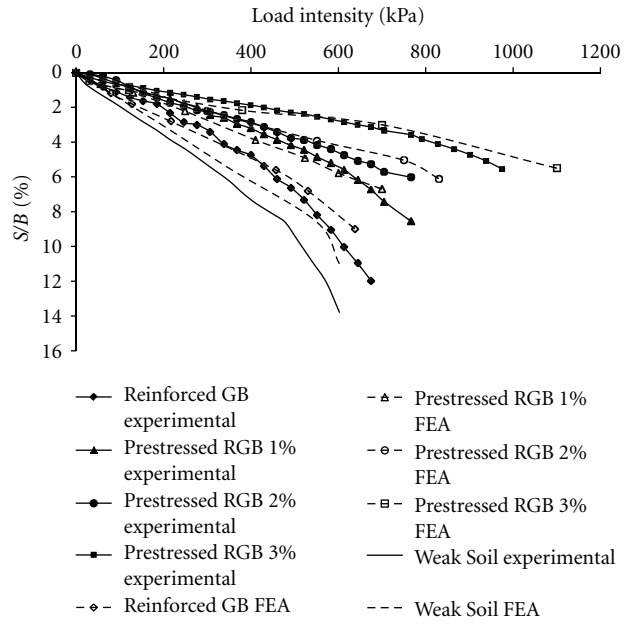

Figure 15: Load intensity versus normalized settlement curves for granular bed of thickness $2B$ with uniaxial prestressing overlying (moist) weak soil 1.

With increased thickness of granular bed to $2B$ and with uniaxial prestressing overlying (submerged) weak soil 2, it is observed (Figure 19) that the maximum improvement is observed when the magnitude of prestress is again equal to 2% of the tensile strength of reinforcement. Further increase in prestress caused a reduction in the improvement in bearing capacity. It is also observed that the improvement

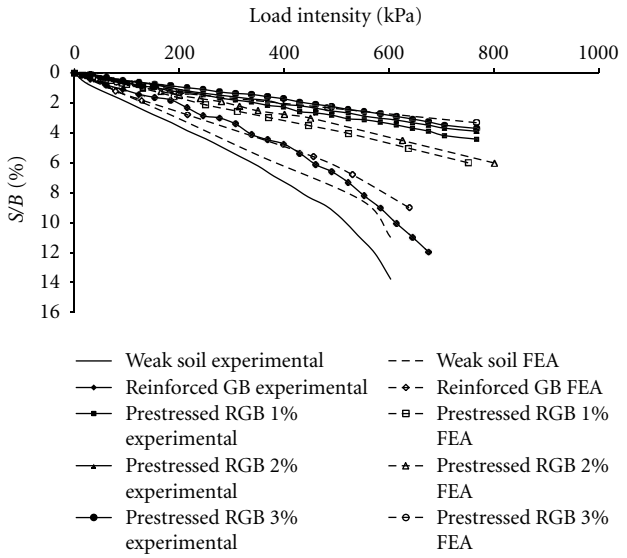

Figure 16: Load intensity versus normalized settlement curves for granular bed of thickness $2B$ with biaxial prestressing overlying (moist) weak soil 1.

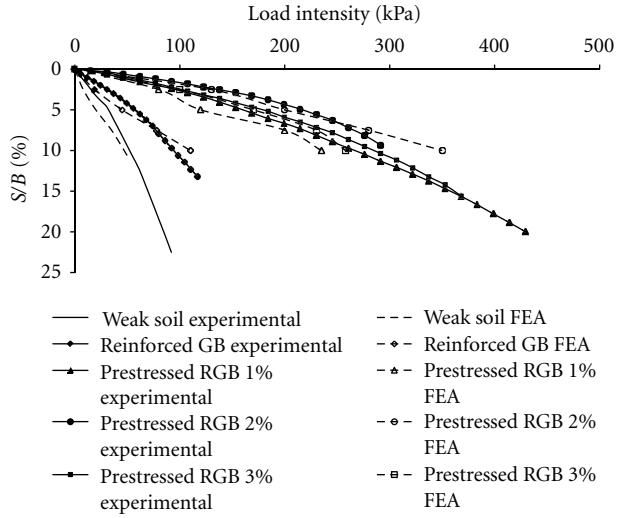

Figure 17: Load intensity versus normalized settlement curves for granular bed of thickness B with uniaxial prestressing overlying (submerged) weak soil 2.

in bearing capacity when the prestress was increased from 1% to 2% was only marginal. With the results obtained from a granular bed of thickness $2B$ with biaxial prestressing overlying (submerged) weak soil 2, it is observed that the improvement in settlement behaviour with 3% prestress is less than that with 1% and 2% (Figure 20). The improvement in settlement behaviour with a prestress of 1% and 2% was almost the same up to a pressure of 370 KPa. At stresses more than 370 KPa, the improvement in settlement behaviour was more than with a prestress of 2%.

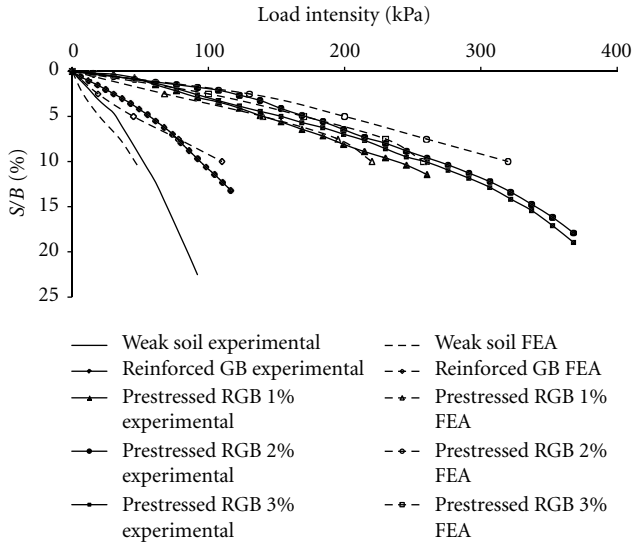

Figure 18: Load intensity versus normalized settlement curves for granular bed of thickness B with biaxial prestressing overlying (submerged) weak soil 2.

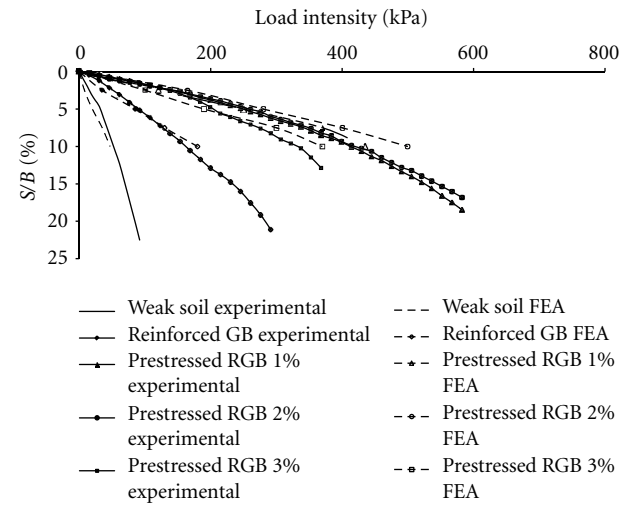

Figure 19: Load intensity versus normalized settlement curves for granular bed of thickness $2B$ with uniaxial prestressing overlying (submerged) weak soil 2.

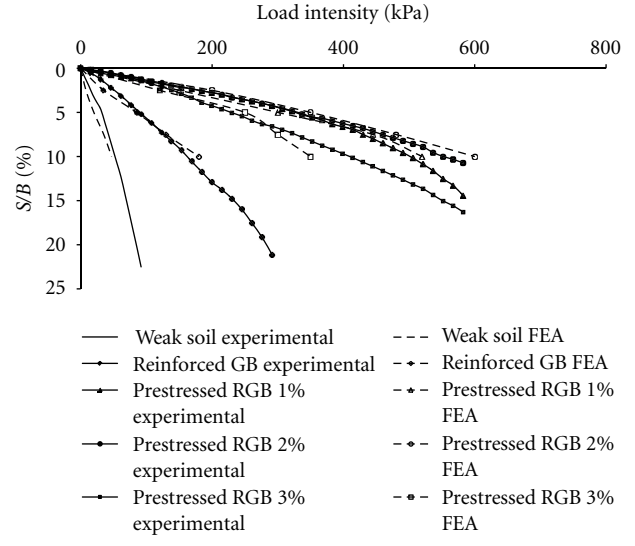

Figure 20: Load intensity versus normalized settlement curves for granular bed of thickness $2B$ with biaxial prestressing overlying (submerged) weak soil 2.

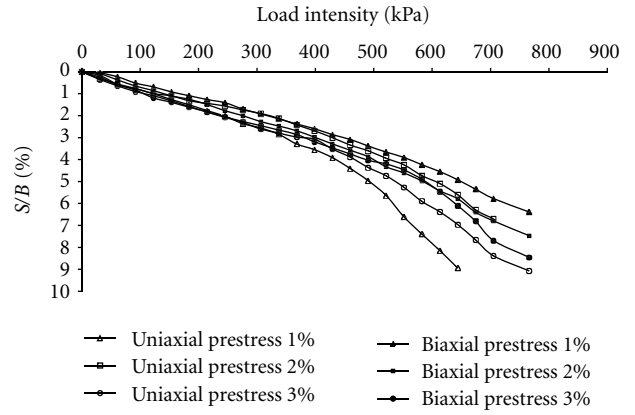

Figure 21: Comparison between load intensity versus normalized settlement curves from experimental results for granular bed of thickness B overlying (moist) weak soil 1 with uniaxial and biaxial prestressing.

5.1.2. Effect of Direction of Prestress

Granular Beds Overlying (Moist) Weak Soil 1. A comparison between the experimentally observed improvements in settlement behaviour of a granular bed of thickness B, overlying (moist) weak soil 1, due to uniaxial and biaxial prestressing is shown in Figure 21. Therein, it is observed that improvement in settlement behaviour is generally more when prestress is biaxial. Maximum improvement in settlement behaviour is observed when the biaxial prestress is equal to 1% of the tensile strength of reinforcement. Figure 22 shows a comparison between the experimentally observed improvements in settlement behaviour of a granular bed of thickness $2B$, overlying moist weak soil, due to uniaxial and biaxial prestressing. In this case, also the general improvement in settlement behaviour is more when prestress is biaxial. Maximum improvement is observed when the prestress is equal to 3% of the tensile strength of reinforcement. It is also observed that when the magnitude of prestress is equal to 3%, the improvements attained due to uniaxial prestressing and biaxial prestressing are almost similar.

Figure 23 shows a comparison between the experimentally observed improvements in settlement behaviour of a granular bed of thickness B, overlying (submerged) weak soil 2, due to uniaxial and biaxial prestressing. In general, the improvement in settlement behaviour is more when prestress is uniaxial. Maximum improvement in settlement behaviour is observed when the uniaxial prestress is equal to 2% of the tensile strength of reinforcement. Further, Figure 24 shows a comparison between the experimentally observed

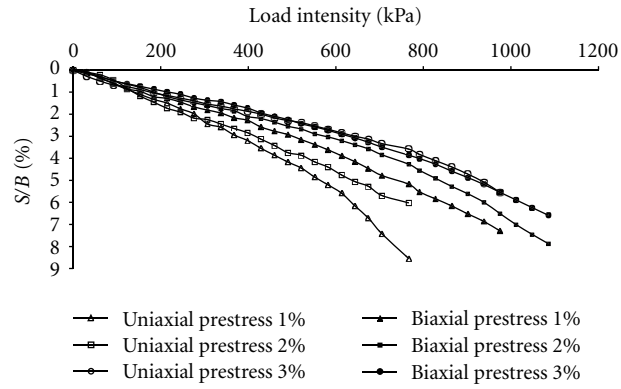

Figure 22: Comparison between load intensity versus normalized settlement curves from experimental results for granular bed of thickness 2*B* overlying (moist) weak soil 1 with uniaxial and biaxial prestressing.

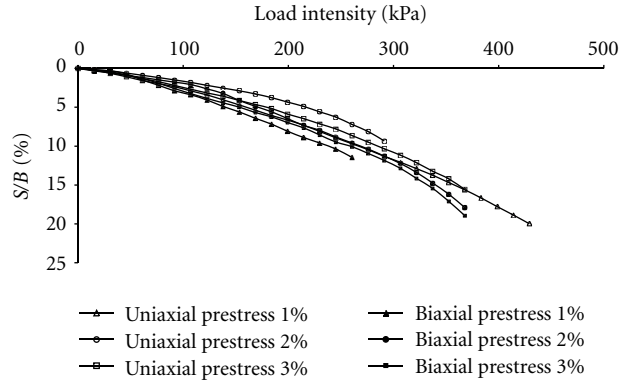

Figure 23: Comparison between load intensity versus normalized settlement curves from experimental results for granular bed of thickness *B* overlying (submerged) weak soil 2 with uniaxial and biaxial prestressing.

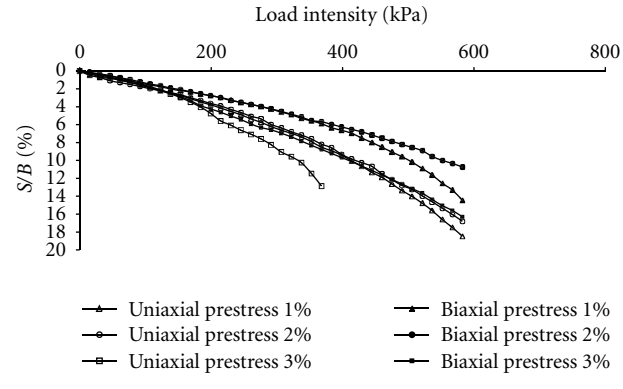

Figure 24: Comparison between load intensity versus normalized settlement curves from experimental results for granular bed of thickness 2*B* overlying (submerged) weak soil 2 with uniaxial and biaxial prestressing.

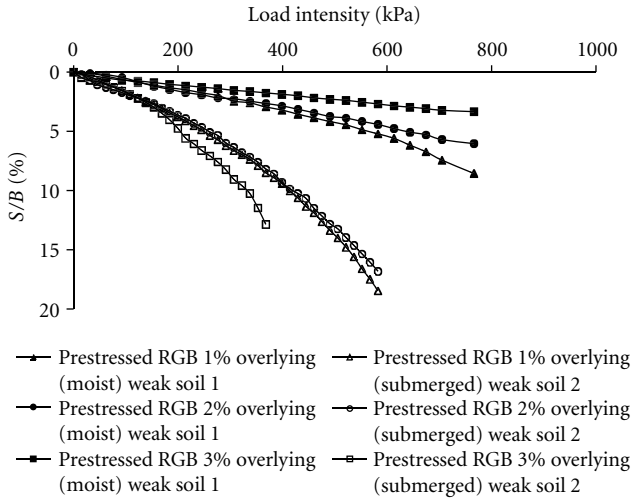

Figure 25: Comparison between load intensity versus normalized settlement curves from experimental results for granular bed of thickness 2*B* with uniaxial prestressing overlying (moist) weak soil 1 and (submerged) weak soil 2.

improvements in settlement behaviour of a granular bed of thickness 2*B*, overlying (submerged) weak soil 2, due to uniaxial and biaxial prestressing. In this case, the general improvement in settlement behaviour is more when prestress is biaxial. Maximum improvement is observed when the biaxial prestress is equal to 2% of the tensile strength of reinforcement.

5.1.3. Effect of Submergence of Shedi Soil. The effect of submergence of soil used in the present study is presented in Figures 25 and 26. Submergence of soil caused a significant reduction in the bearing capacity. Submerged soil (weak soil 2) generally gave better results at 2% prestressing force for both thickness of granular bed, namely, *B* and 2*B*. However, for the comparatively stronger soil (weak soil 1), a greater prestressing force of 3% was required for thickness of 2*B* for both uniaxial and biaxial prestressing.

5.2. Settlement Measurement at the Interface after Test in Case of (Moist) Weak Soil 1. The distribution of settlement at the interface between sand and (moist) weak soil 1, in a granular bed of thickness *B*, subjected to uniaxial and biaxial prestressing is given in Figure 27. In general, the settlement of the underlying weak soil is lesser in case of biaxial prestressing than uniaxial prestressing. The settlement of weak soil is found to be the least when the biaxial prestress is equal to 3% of the tensile strength of reinforcement.

The interface settlement along the direction of prestress and along its perpendicular direction during uniaxial prestressing of a granular bed of thickness *B* is presented in Figure 28. It is observed that along the direction of prestress, the interface settlement is distributed on a wider area than in the cross direction. The interface settlement is, in general, lesser in the cross direction than the prestressed direction, even though the peak interface settlement is equal for both cases. This supports the presumption made in Section 3.3.3.

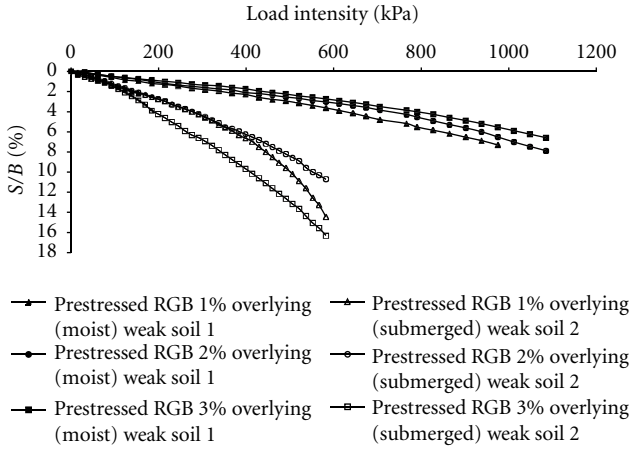

Figure 26: Comparison between load intensity versus normalized settlement curves from experimental results for granular bed of thickness $2B$ with biaxial prestressing overlying (moist) weak soil 1 and (submerged) weak soil 2.

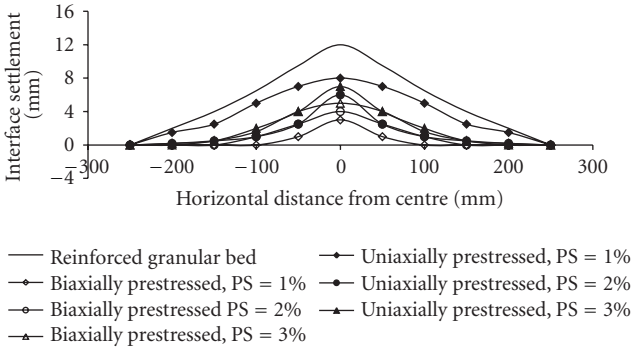

Figure 27: Distribution of settlement at the interface between RGB and (moist) weak soil 1 when thickness of granular bed is B.

5.3. Numerical Analysis. All the above various cases were analysed numerically using the model proposed. The bearing capacity ratios obtained experimentally and predicted by the model are shown graphically in Figure 29. It is observed that the model predicts the bearing capacity ratios with good accuracy for all the cases.

6. Conclusions

Based on the results obtained from experimental and numerical studies, the following conclusions are made on the behaviour of prestressed reinforced granular beds overlying weak soils.

(1) The addition of prestress to geonet reinforcement significantly improves the bearing capacity and settlement behaviour of the soil.

(2) The improvement in bearing capacity depends on the thickness of granular bed, magnitude of prestress, and the direction of prestress. The improvement in bearing capacity is found to be more with biaxial prestressing than uniaxial prestressing. Settlements are also less with biaxial prestressing. The improvement in bearing capacity increases with the thickness of granular bed.

(3) Prestressing of reinforcement significantly reduces the settlement of the underlying weak soil.

(4) Biaxial prestressing works better with thicker granular beds.

(5) The numerical model proposed in this study predicts the bearing capacity ratios for all the cases with good accuracy.

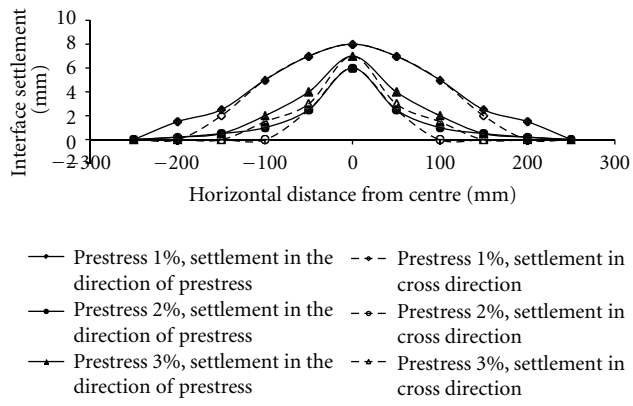

Figure 28: Distribution of settlement at the interface between RGB and (moist) weak soil 1, in the direction of prestress and in its perpendicular direction, for granular bed of thickness B, when prestress is uniaxial.

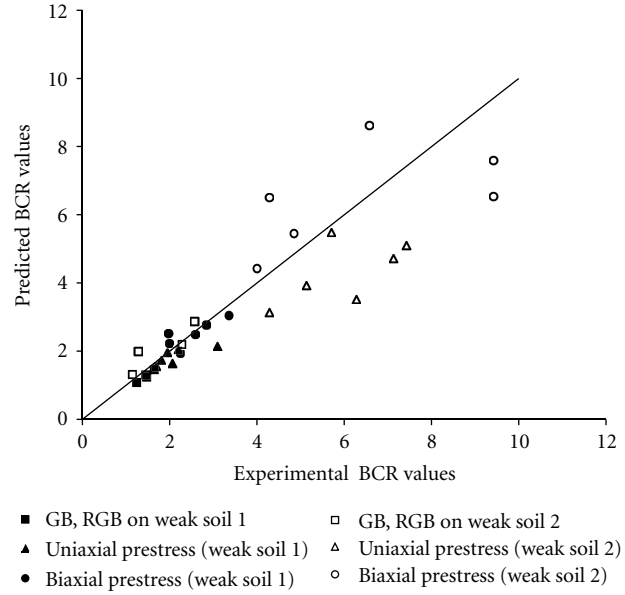

Figure 29: Comparison between observed and predicted values of bearing capacity ratios for granular beds overlying (moist) weak soil 1.

(6) The results obtained from finite element analyses are in reasonably good agreement with the experimental results.

(7) To prestress the reinforcement in the field, the geosynthetic should be pulled out with the required force and anchored by driving soil nails or by any other suitable method. Further study is required to determine the effects of any losses in prestress due to anchorage slip, stress relaxation in reinforcement, shrinkage of soil, and so forth.

References

[1] G. L. Sivakumar Babu, *An introduction to Soil Reinforcement and Geosynthetics*, Universities Press, 2006.

[2] J. Binquet and K. L. Lee, "Bearing capacity tests on reinforced earth slabs," *Journal of Geotechnical Engineering*, vol. 101, no. 12, pp. 1241–1255, 1975.

[3] R. Shivashankar, M. R. Madhav, and N. Miura, "Reinforced granular beds overlying soft clay," in *Proceedings of the 11th South East Asian Geotechnical Conference*, pp. 409–414, Singapore, 1993.

[4] N. P. Kurian, K. S. Beena, and R. Krishna Kumar, "Settlement of reinforced sand in foundations," *Journal of Geotechnical and Geoenvironmental Engineering*, vol. 123, no. 9, pp. 818–827, 1997.

[5] K. Deb, S. Chandra, and P. K. Basudhar, "Nonlinear analysis of multilayer extensible geosynthetic-reinforced granular bed on soft soil," *Geotechnical and Geological Engineering*, vol. 25, no. 1, pp. 11–23, 2007.

[6] K. Deb, N. Sivakugan, S. Chandra, and P. K. Basudhar, "Numerical analysis of multi layer geosynthetic-reinforced granular bed over soft fill," *Geotechnical and Geological Engineering*, vol. 25, no. 6, pp. 639–646, 2007.

[7] S. Alamshahi and N. Hataf, "Bearing capacity of strip footings on sand slopes reinforced with geogrid and grid-anchor," *Geotextiles and Geomembranes*, vol. 27, no. 3, pp. 217–226, 2009.

[8] G. Madhavilatha and A. Somwanshi, "Bearing capacity of square footings on geosynthetic reinforced sand," *Geotextiles and Geomembranes*, vol. 27, no. 4, pp. 281–294, 2009.

[9] G. Madhavilatha and A. Somwanshi, "Effect of reinforcement form on the bearing capacity of square footings on sand," *Geotextiles and Geomembranes*, vol. 27, no. 6, pp. 409–422, 2009.

[10] R. Sharma, Q. Chen, M. A. Farsakh, and S. Yoon, "Analytical modeling of geogrid reinforced soil foundation," *Geotextiles and Geomembranes*, vol. 27, no. 1, pp. 63–72, 2009.

[11] P. Vinod, A. B. Bhaskar, and S. Sreehari, "Behaviour of a square model footing on loose sand reinforced with braided coir rope," *Geotextiles and Geomembranes*, vol. 27, no. 6, pp. 464–474, 2009.

[12] J. Lovisa, S. K. Shukla, and N. Sivakugan, "Behaviour of prestressed geotextile-reinforced sand bed supporting a loaded circular footing," *Geotextiles and Geomembranes*, vol. 28, no. 1, pp. 23–32, 2010.

[13] A. P. S. Selvadurai, *Elastic Analysis of Soil-Foundation Interaction*, Elsevier Scientific Publishing Company, New York, NY, USA, 1979.